Self-Assembly and Vortices Formed by Microparticles in Weak Electrolytes

M. V. Sapozhnikov,[1,2] I. S. Aranson,[1] W.-K. Kwok,[1] and Y. V. Tolmachev[1,3]

[1]*Materials Science Division, Argonne National Laboratory, 9700 South Cass Avenue, Argonne , Illinois 60439, USA*
[2]*Institute for Physics of Microstructures, Russian Academy of Sciences, GSP-105, Nizhny Novgorod, 603000, Russia*
[3]*Department of Chemistry, Kent State University, Kent, Ohio 44242, USA*

We carried out experimental studies of the self-assembly of metallic micron-size particles in poorly conducting liquid subject to a constant electric field. Depending on the experimental conditions, the particles self-assemble into long chains directed along the electric field lines and form vortices and other structures. The vortices perform Brownian-type random motion due to self-induced chaotic hydrodynamic flows. We measured the diffusivity constant of the vortices and the conductivity and mechanical stiffness of the chains.

Understanding the unifying principles of the self-assembly of complex systems such as macromolecules [1], diblock copolymers [2], micromagnetic systems [3], ensembles of charged particles [4] is the key to future advances in nanoscience. The electric field-driven self-assembly of colloidal particles in clusters and lattices in aqueous solutions (so-called strong electrolytes) has received increased attention in recent years due to its possible applications in bioanalysis, micro- and nanofabrication. Aqueous solutions have small (of the order of a few nanometers) Debye length and negligible deviations from bulk electroneutrality. In contrast, nonaqueous solutions or weak electrolytes, which are often characterized by anomalously thick Debye layers, small conductivity and significant deviation from bulk neutrality, remains poorly understood. Low conductivity of nonaqueous solutions allows the application of a strong electric field without substantial heating and electrolysis, a condition often impossible to attain in strong electrolytes. Whereas in aqueous solutions direct electrostatic interaction between the particles is negligible due to strong Debye screening effects, in nonaqueous systems this electrostatic interaction is often the dominant one, and opens the possibility to tune the resulting particle patterns by adjusting the amplitude and frequency of the applied field. In our previous work we focused on self-assembly and pattern formation of relatively large (120 μm bronze) particles in weakly conducting liquid (toluene-ethanol mixtures) [5]. Our research yielded a rich variety of self-organized dynamic structures of metallic particles, from honeycombs and two-dimensional crystals to pulsating rings and rotating multipetal vortices.

In this Letter we report experimental studies of electric field induced self-assembly of micron-size conducting particles. The particles size reduction results in an overall decrease of the self-organized pattern scale and a qualitatively different relationship between the primary interactions which control the dynamics of self-assembly: gravity, electric and hydrodynamic forces. Consequently, the microparticles assemble into qualitatively different structures not previously observed in experiments with larger particles. We discovered a new class of vortex objects and self-assembled chains formed by micron-size silver particles in a constant (dc) electric field. The vortices perform random motion due to self-induced chaotic electrohydrodynamic flow. The formation of chains can be explained by charge exchange between the metallic particles and the surrounding liquid.

The design of our experimental cell is similar to that reported earlier [6]. We used dry silver powder (Aldrich, product No. 32708-5) consisting of 20–30 μ conglomerates of 2.5 $\pm$ 0.5 μm particles. Experiments performed with gold particles (1.5–3 μm Alfa Aesar, product No. 39818) yield qualitatively similar results. To split the conglomerates and to prepare a single-particle suspension, the powder was treated about 30 min in an ultrasonic bath in a saturated 1-hexadecylpyridinium bromide solution in toluene. The suspension was then placed in a toluene-ethanol mixture and injected into a 0.25–0.75 mm gap between two horizontal electrodes formed by glass plates coated by a transparent conducting layer of indium-doped tin oxide (in what follows, we refer to this setup as a "vertical cell" because the electric field direction is parallel to the gravity). In the most of experiments the volume fraction of the particles was very small (about 0.1%). Some experiments were also performed in a "horizontal cell" formed by two horizontal copper electrodes sandwiched between two glass plates for optical access in the direction perpendicular to the electric field. The presence of ethanol allows adjustment of the conductivity of the mixture in the range of 5×10^{-9}–5×10^{-7} Ohm^{-1} m^{-1}, which is still about 8–9 orders of magnitude smaller than the conductivity of typical aqueous electrolytes. A homogeneous electric field of up to 10 kV/cm was created inside the cell. The real time motion of the particles was monitored by a high-speed camera attached to a microscope with micron resolution.

The operation of the electrostatic cell is described in detail in Refs. [5–7]. The application of an electric field induces the particles in the cell to acquire an electric charge due to contact with the bottom electrode. When the dc electric field exceeds a certain critical value E_1 in the vertical cell, the particles begin to move upward because the resulting upward force induced by the electric field exceeds the gravitational and the adhesion force. When the particles reverse their charge upon contact with the upper electrode, they are repelled back down to the bottom electrode. This process repeats in a cyclical fashion while the dc electric field is applied.

The above situation changes with the addition of ethanol (above 2.5% v/v) into toluene solution: upon gradual increase of the electric field the particles first migrate to the negative electrode, even if this electrode is the top one. This phenomenon can be explained by the presence of excess negative charge in the bulk of the fluid, and therefore, the apparent electric field experienced by the particles is always larger in the vicinity of the positive electrode. This violation of electroneutrality can be explained by the asymmetry of the electrochemical reaction rates. Namely, the production rate of negative ions (most likely $C^2H^5O^-$ and OH^-) at the negative electrode exceeds the corresponding production rate of H^+ ions at the positive electrode. Moreover, the positive H^+ ions are more likely to be adsorbed on the electrodes, whereas the negative ions are distributed throughout the cell by the electric current. Experimental estimates show that the liquid contains almost exclusively ions of the same (negative) sign (albeit at a very small concentration, 10^{16} m^{-3} for 3% ethanol concentration) [5]. We have found that the particles often discharge in the bulk of the fluid. For moderate values of the field E one observes that the majority of the particles are reversed back somewhere in the middle of the cell even without touching the upper electrode Fig. 1(a).

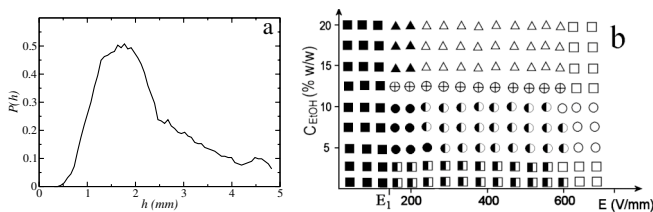The phase diagram delineating the primary experimental regimes for a vertical cell as a function of applied electric field E and concentration of ethanol c is shown in Fig. 1(b). For an ethanol concentration above 5% the particles begin to form clusters at the negative electrode, see Fig. 2(a). The system of clusters possesses a short-range hexatic order similar to Refs. [8]. The distance between clusters appears to be proportional to the gap between the plates. Increasing the electric field causes some particles in the cluster to begin to bounce between the cluster and the opposite plate, thereby and creating a dynamic toroidal vortex structure [Fig. 2(b)]. The particle flow at the central axis of the toroid is from the negative to the positive electrode. These vortices are similar to that formed by larger particles reported in Ref. [5]. However, in our case the center of the vortex (vortex core) exhibit random motion in horizontal plane. With the increase of electric field the clusters evaporate and all particles become involved in the vortical motion, Fig. 2(c). A typical trajectory of the vortex core motion in the horizontal plane and the dependence of the vortex core diffusivity on applied voltage are shown in Fig. 3.

Further increase of the ethanol concentration leads to a new surprising transition in the vortex structure: the vortices start to be formed by chain segments of connected particles growing from the cluster in the center of the vortex. These chain segments persist even after switching off the electric field and can be observed lying at the bottom electrode with the optical microscope. For ethanol concentration of the order of 15–20% v/v, the size of the overall vortex gradually decreases and long chains of particles begin to grow spontaneously from the negative electrode, Fig. 4(a). These chains have single-particle thickness, see Fig. 4(b). For higher electric field values the chains become unstable and dynamic "tree-like" structures begin to form: particles become detached from the end of the chain and reattach to the middle, see Fig. 5. A further increase of the field leads to eventual breakdown of the chains and the particles begin to bounce separately.

The overall picture bears a strong resemblance to that of macroscopic particles, Ref. [5]. For example, similar toroidal vortices were observed with larger particles as well. However, a very sharp difference occurs due to
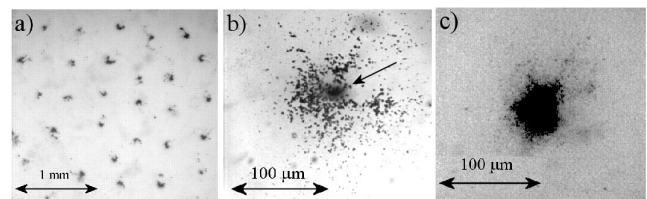

FIG. 1. (a) Distribution function $P(h)$ of particles jumps vs height h for 120 μm particles, $E = 160$ V/mm, concentration of ethanol 7%, gap between electrodes 5 mm. (b) Phase diagram: immobile particles for $E < E_1$ (solid squares); gas of bouncing particles (open squares); coexistence of bouncing and immobile particles (half-solid squares); lattice of clusters (solid circles); vortices (open circles), vortices above clusters (half-solid circles); vortices formed by chain segments (crossed circles); chains (solid triangles); branched chains (triangles).

FIG. 2. (a) Lattice of clusters, $E = 200$ V/mm, $c = 7.5\%$ v/v; (b) cluster with vortex above it. The arrow indicates the core, $E = 350$ V/mm, $c = 7.5\%$ v/v; (c) diffusing vortex consisting of moving particles only, $E = 600$ V/mm, $c = 7.5\%$ v/v. E is perpendicular to the plane of images.
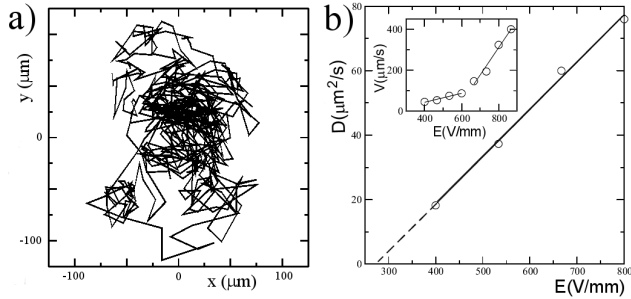
FIG. 3. (a) Trajectory of the vortex core for $E = 600$ V/mm, $c = 7.5\%$ v/v. (b) Diffusivity D and typical velocity of the core V vs E for $c = 7.5\%$ v/v.

reduced particle size. In the "macroscopic cell" (cell with 120 μm Bronze particles) the phase diagram is asymmetric with respect to the direction of the electric field due to the close competition between gravitational and electric forces. In the "microscopic cell" (2 μm particles) gravity is negligible compared to the electric forces, and the phase diagram is practically symmetric with respect to the applied field. Reversal of the field direction results in the development of the same type of phenomena at the upper electrode instead of the bottom one. Moreover, the hydrodynamic effects become even more profound for reduced particle sizes due to the increased role of the viscous drag force.

The formation of the cluster lattices and toroidal vortices are likely caused by the same mechanism: self-
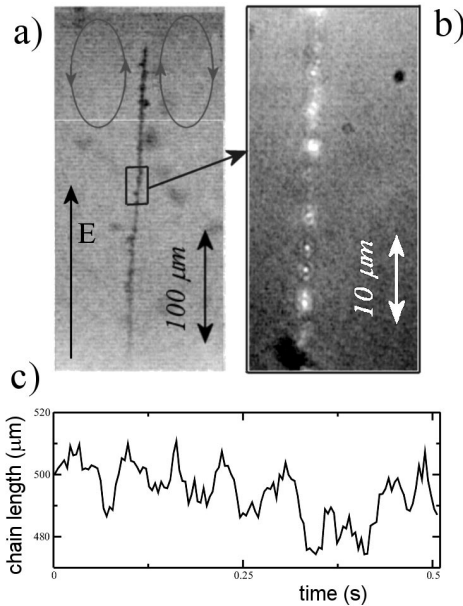

FIG. 4. (a) Self-assembled chains at $E = 150$ V/mm and $c = 15\%$ v/v. Electrohydrodynamic vortices are indicated by arrows; (b) magnification of the chain segment; (c) oscillations of the chain length vs time.

induced vortical electrohydrodynamic flows in the vicinity of particles [4,5,9,10]. These electrohydrodynamic flows facilitate self-assembly of particles in various macroscopic structures.

We studied the time evolution of the core positions using a high-speed video-microscope. The mean squared displacement of the core against time is shown in Fig. 3(b). The typical velocity of the vortex core $V = \langle \sqrt{v_x^2 + v_y^2} \rangle$ is shown in the inset to Fig. 3. As one sees from the figure, over a wide range of parameters, the vortex core exhibits Brownian-type motion characterized by the diffusion coefficient D. The value of D depends strongly on the applied electric field ruling out the origin of diffusion due to molecular thermal motion. The abrupt change of slope in the dependence of V versus the applied electric field at $E \approx 600$ V/mm corresponds to the transition from vortices existing above the cluster of almost immobile particles [Fig. 2(b)] to "free" vortices shown in Fig. 2(c). It is quite likely that the cluster "pins" the vortex core and reduces its mobility. We also anticipate that the primary reason for vortex diffusion is chaotic electrohydrodynamic flows induced by the moving particles. This effect is practically absent in larger particles because of the reduced viscous drag effect. Since viscous drag is proportional to the particle size a, electric force is proportional to a^2 (see [6]), and gravitational force is proportional to a^3, the dynamics of very small particles will be largely determined by the balance between viscous drag and electric forces while gravity is negligible.

For higher ethanol concentrations the vortices gradually give way to chains. Adhesion between particles maintains the chain's stability even after the electric field is switched off, allowing their conductivity to be measured (conductivity measurements were actually performed in the horizontal cell). For 1 mm chains, the conductivity is in the range of 3–4.5 kOhm/mm. It implies that the individual grain has effective resistance of the order of 10 Ohm, strongly suggesting a tunnelling nature for the conductivity. Eventually, the fluid can be
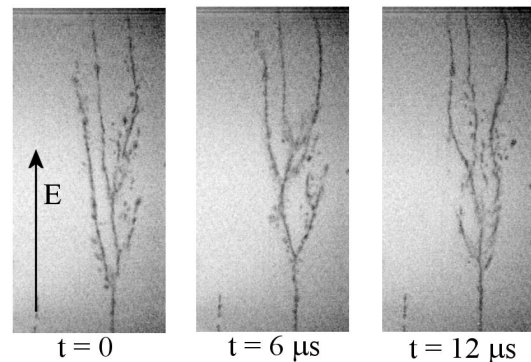

FIG. 5. Time evolution of branched chain state, $E = 250$ V/mm, $c = 15\%$ v/v.

drained from the cell and the formed chains can be deposited onto a dielectric substrate. These chains can be possibly used for various nanotechnological applications, e.g., microsensors based on beaded wires [11].

In a constant electric field, the length of the chain oscillates with a characteristic frequency $f \sim 16$ Hz, Fig. 4(c). These oscillations are manifestations of the competition between hydrodynamic and electric forces. Using the analogy between chain oscillations and harmonic mechanical vibrations of a spring with mass m and spring constant k, one can estimate the effective spring constant of a chain of about 300 particles. Thus, the effective spring constant of a chain of about 300 particles (mass $m \times 2 \times 10^{-8}$ g) is $k = 4\pi^2 f^2 m \sim 2 - 3 \times 10^{-7}$ N/m. Therefore, for an absolute chain extension of about 20 μm, one estimates the attractive force between particles to be about 4 pN, a value comparable to the 2–6 pN force created by adenosine triphosphate molecular motors [12].

The formation of chains resembles some features of the electrorheological response of dielectric colloidal particles in nonaqueous solutions; see, e.g., [13,14]. As in colloidal suspensions, the chains are formed along the electric field lines. However, in the electrorheological fluid the aggregation is caused by the induced electric dipole interaction and occurs in the bulk of the fluid. In our case the chain formation is caused by self-induced electrohydrodynamic flows and is facilitated by the charge exchange between conducting particles and the surrounding liquid via an electrochemical reaction; see Fig. 1(a). Since the particles in the chain have electric charges of the same sign, the electric field favors disintegration of the chain. However, if a particle tears off from the end of a chain, it eventually recharges in the bulk of the conducting liquid and is brought back to the chain by the electric field. The formation of single-particle-width chain is assisted by the circulating electrohydrodynamic vortices generated in the vicinity of the free end of the chain, Fig. 4(b). These vortices, observed in our experiments by tracking of individual particle trajectories, exert a viscous drag force on nearby particles and concentrate them towards the end of the chain, consequently keeping the chain intact. The formation of chains is possible at high enough concentrations of ethanol in the solution when the conductivity of the liquid is high sufficient to rapid particle discharge. Thus, in our case the chain formation is more complicated than that of the ordinary electrorheological fluids: the chains always grow from the negative electrode, exhibit dynamic oscillations and structural instabilities not observed in dielectric colloidal suspensions. At even higher E values novel instability resulting in formation of branched chains is observed, see Fig. 5: short chain segments torn off from the end of the main chain succeed to reach the positive electrode whereupon they recharge on contact. Subsequently, these segments are advected by the surrounding vortices towards the middle of the chain, where they become reattached.

The theoretical description of the vortices is similar to that proposed in our earlier work [15] based on a phenomenological set of equations for the coarse-grained number densities of bouncing and immobile particles coupled to self-induced electrohydrodynamic flows. However, the chains require an entirely different approach because these single-particle wide objects cannot be adequately addressed in the framework of a continuum model for coarse-grained densities.

We report the discovery of a series of novel vortex phases and self-assembled dynamic chains of electric field-driven conductive microparticles in poorly conductive fluids. Our results exemplify the importance of self-induced hydrodynamic interactions between the particles and uncompensated ionic charges in the bulk of the liquid. Extension of our experiments towards self-assembly of submicron and nano particles may result in a totally new approach for fabrication of metallic nanowires and chains. Application of our technique to magnetic and anisotropic particles may result in even more surprising collective phenomena.

[1] E. Winfree *et al.*, Nature (London) **394**, 539 (1998).
[2] W. A. Lopes and H. M. Jaeger, Nature (London) **414**, 735 (2001).
[3] S. I. Woods *et al.*, Phys. Rev. Lett. **87**, 137205 (2001).
[4] R. C. Hayward, D. A. Saville, and I. A. Aksay, Nature (London) **404**, 56 (2000).
[5] M. V. Sapozhnikov, Y. V. Tolmachev, I. S. Aranson, and W.-K. Kwok, Phys. Rev. Lett. **90**, 114301 (2003).
[6] I. S. Aranson *et al.*, Phys. Rev. Lett. **84**, 3306 (2000).
[7] I. S. Aranson *et al.*, Phys. Rev. Lett. **88**, 204301 (2002).
[8] D. Grier and C. Murray, in *Ordering and Phase Transitions in Charged Colloid*, edited by A. K. Arora and B. V. R. Tata (VCH Publishers, N.Y., 1996); B. V. R. Tata *et al.*, Phys. Rev. Lett. **84**, 3626 (2000).
[9] M. Trau *et al.*, Nature (London) **374**, 437 (1995).
[10] Y. Solomentsev, M. Böhmer, and J. L. Anderson, Langmuir **13**, 6058 (1997).
[11] F. Favier *et al.*, Science **293**, 2227 (2001).
[12] H. Higuchi *et al.*, Proc. Natl. Acad. Sci. U.S.A. **94**, 4395, (1997).
[13] A. P. Gast and C. F. Zukoski, Adv. Colloid Interface Sci. **30**, 153 (1989); A. Bezryadin, R. M. Westervelt, and M. Tinkham, Phys. Rev. E **59**, 6896 (1999); T. C. Halsey and W. Toor, Phys. Rev. Lett. **65**, 2820 (1990).
[14] T. B. Jones, *Electromechanics of Particles* (Cambridge University Press, Cambridge, 1995).
[15] I. S. Aranson and M. V. Sapozhnikov, Phys. Rev. Lett. **92**, 234301 (2004).